Proceedings of the ASME 32nd International Conference on Offshore Mechanics and Arctic Engineering
OMAE2013
9th- 14th June 2013, Nantes, France

OMAE2013- 11467

DYNAMICS OF ENTRAPPED WATER IN LARGE DIAMETER TURRET MOONPOOLS

Igor de Vries[(1)], Yann Roux[(2)], Mamoun Naciri[(1)] & Guillaume Bonnaffoux[(1)]

[(1)] SBM Offshore
24 Avenue de Fontvieille BP199
MC98007 Monaco Cedex
Igor.devries@sbmoffshore.com

[(2)] K-Epsilon
300 Route des Crètes
06560 Sophia-Antipolis
yann@k-epsilon.com

Keywords:
FPSO, Turret, Moonpool, Resonance, CFD, Piston, Sloshing, Radiation/diffraction.

ABSTRACT

Development of Turret Mooring Systems (TMS) for harsh environment and large number of risers has led to a drastic increase of the size of the chaintable and consequently of the turret cylinder diameter. Furthermore, harsh environments usually require relatively deep drafts. As a consequence, the volume of entrapped water in large turrets increases to levels never designed for before. In some cases, the mass of the entrapped water can be comparable to the turret mass. Whilst this entrapped water does not exert any weight on the weathervaning system, its acceleration due to ship motions induces inertia loads which could affect the balance of loads. Estimation of these inertia loads is easily carried out assuming the entrapped water as frozen. However, to what extent is this assumption valid in view of the large amount of entrapped water involved and of the extreme ship motions expected in harsh environments? Should we expect sloshing of the entrapped water? In this paper, insights will be drawn from numerical techniques of diverse complexity. This will be preceded by a brief literature review on sloshing in moonpools. Practical analysis and design recommendations will be proposed. Operational aspects related to installation will be covered as well.

1. INTRODUCTION

The development of Turret Mooring Systems for harsh environments and large number of risers has led to an ever increasing turret cylinder diameter. In addition, the severe metocean environments drive relatively deep drafts. The above results in larger and larger amounts of water being trapped in the turret moonpool as shown in Figure 1-1 hereafter.

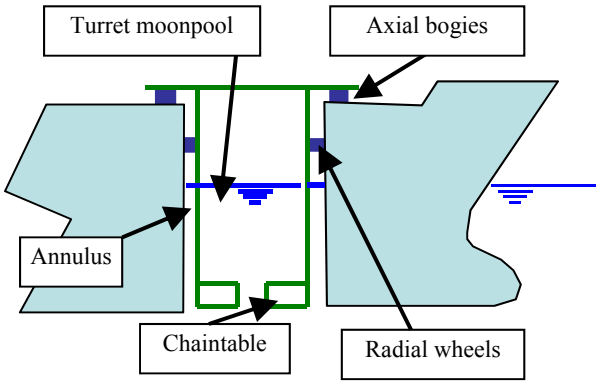

Figure 1-1 Schematic of turret

Trapped fluids within a floating body are rather common; all crude oil carriers and LNG carriers are subjected to fluid motions (and associated loads) within their holds. The originality of the situation illustrated above is that the fluid is seawater and that it is in not fully trapped within the moonpool but rather is susceptible to flow in and out of this moonpool as a result of ship motions and direct wave action.

Moonpool-related issues have been investigated for many years for drill ships. These issues include increased resistance in forward speed due to the opening in the hull meaning longer transit durations; agitation in the moonpool during both transit and drilling operations with associated risks to on-board personnel. The geometry of drillship moonpools is rarely cylindrical and their position is usually close to amidships to minimise heave motions

unlike turret moonpools. In view of these differences, the moonpool review in the next section will omit drillship related literature.

A literature review of moonpool related issues in relation to floating systems without forward speed is presented in §2. Recent trends in turret systems executed by SBM during the past fifteen years will be described in §3 to illustrate the general context of the current work. In the next section, insights from radiation/diffraction analyses will be presented. Free surface decay numerical experiments of various complexity are described in §5. Entrapped water and related turret loads are described in §6. Guidelines for incorporation of entrapped water effects are proposed in §7 before drawing conclusions and suggesting areas worthy of further attention in §8.

2. LITERATURE REVIEW

The concept of a moonpool is no stranger to the Oil and Gas Industry. The drillship has been mentioned before. The widespread Catenary Anchor Leg Mooring (CALM) system is another example of floating structure with a moonpool. In contrast with drillships, the moonpool in a CALM system is cylindrical.

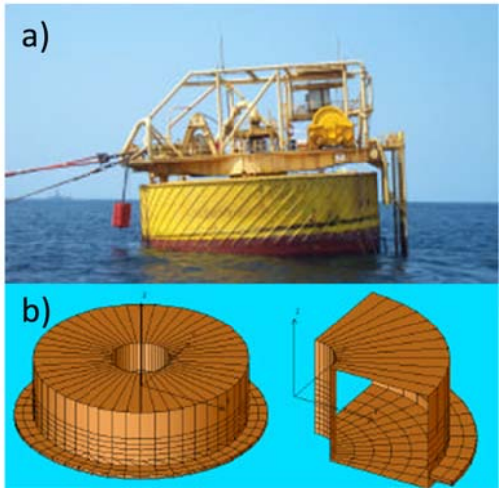

Figure 2-1 a) CALM system b) Diffraction model showing moonpool

Radiation/diffraction analysis of a CALM system shows a sudden sign change of the heave added mass and a large jump in the heave radiation damping at a specific frequency ω_o (see Ref [1]). A wavenumber k_o is associated with ω_o through the dispersion relation. Such phenomenon has been demonstrated for a class of three dimensional bodies later referred to as the McIver toroid (see Figure 2-2 hereafter) to be related to the existence of a homogeneous solution of the linear water wave radiation problem at a specific frequency (Ref [2]). Radiation/diffraction analyses with WAMIT demonstrated that unlike irregular frequencies, the abovementioned phenomenon was physical (Refs [3] and [4]). Interestingly, it is shown for the McIver toroid that the wavenumber k_o converges linearly with 1/N where N is the number of diffraction panels used to discretize the toroid.

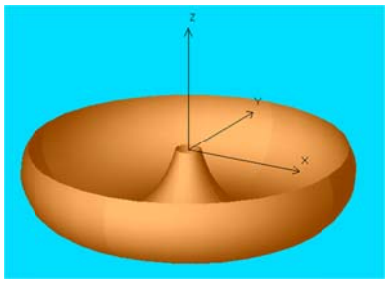

Figure 2-2 McIver toroid (from Ref [3])

Ten to fifteen years ago, a number of Oil Majors were interested in developing FPDSO (Floating Production, Drilling, Storage and Offloading) concepts. The main advantage foreseen at the time was the ability to start production from a limited number of pre-drilled wells – thus accelerating revenues and returns on investment. The remaining drilling activities were to be carried out directly from the FPDSO e.g. without resorting to expensive drilling rigs. The drilling and production risers where either top tensioned by buoyancy tanks located in a large moonpool for the Wellhead Barge (see Ref [5]) or by weights with the Tension Leg Deck system (see Ref [6]). In either case large rectangular moonpools are required in the vicinity of the new-built barge amidships. The dimensions of these moonpools were much greater than ever seen before in drillships or Diving Support Vessels. Understanding the dynamics of the surface elevations in the large moonpool was particularly critical for buoyancy-based top tensioned risers. This has triggered numerous investigations both theoretical and experimental. The piston mode corresponds to the uniform harmonic heaving motion of the free surface. Sloshing modes correspond to spatially periodic oscillations in the longitudinal and transverse moonpool directions.

In Ref [7], the expression of the piston mode natural frequency of a rectangular moonpool with vertical walls is presented as a function of length, width and draft *h*. The expression valid for deep water further assumes a rigid lid boundary condition at $z=-h$ for all x and y except at the moonpool opening in order to obtain a closed semi-analytic solution. In other words, the accuracy of the estimate is better when the horizontal dimensions of the barge are large compared to those of the moonpool. In the case of a moonpool with a square cross section of side *b* and draft *h* the piston mode natural frequency is as follows:

$$\omega_o = [g/(h+0.473b)]^{1/2} \qquad (1)$$

The above work was extended to include as well sloshing modes within the same rectangular moonpool still assuming a barge of infinite horizontal extent to allow semi-analytic expressions to be derived (see Ref [8]). A further extension (see Ref [9]) considers moonpools with slowly varying cross sections in the vertical direction and

provided an approximation of the piston mode wavenumber K:

$$K = \left(S_f \int_{z_b}^{z_f} \frac{dz}{S(z)} + \frac{8R_b}{3\pi}\frac{S_f}{S_b} \right)^{-1} \quad (2)$$

where indices *b* and *f* refer respectively to the bottom and free surface elevations, R and S refer respectively to moonpool z-dependent radius and cross section. The above expression reduces to the following simpler form in the case of a uniform cylindrical moonpool and deep water:

$$\omega_o = [g/(h+8R/3\pi)]^{1/2} \quad (3)$$

Interestingly, a structure with two concentric moonpools is also considered as shown in Figure 2-3. The two zero crossing of the added mass curves demonstrate the existence of two resonant piston modes. This geometry shares with that in Figure 1-1 the presence of two concentric axi-symmetric moonpools.

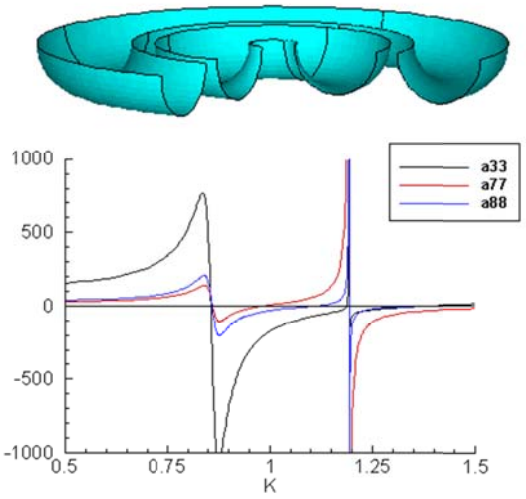

Figure 2-3 Top: Structure with two concentric moonpools. Bottom:a33 heave added mass of entire structure; a77 and a88 respectively heave and radial motion of inner structure alone (from Ref [9])

Numerous model test campaigns have been performed on the Wellhead barge. In Ref [10], regular and irregular wave tests are performed for head, bow-quartering and beam incidences. Relative wave elevations are measured at several location in the large rectangular moonpool. Barge motions and relative wave elevation RAOs are derived from the measurements and compared to predictions from a linear diffraction radiation program. The location of RAO peaks is further examined in light of the quasi-analytical predictions of longitudinal and transverse sloshing mode frequencies as per Ref [8]. A match is found for the 1st longitudinal and 1st transverse sloshing modes. The piston mode is not discussed.

The same barge with rectangular moonpool is used to investigate the piston mode (Ref [11]). Natural periods of piston mode are estimated based on Ref [8], numerical simulations of free surface decay without and with real fluid effects and free surface decay model tests. Quasi-analytic results and real fluid numerical predictions were respectively within 5% and 2% of measurements for the three barge drafts considered. A linear plus quadratic damping model is fitted to the various decay simulations. A better agreement is found for the linear damping (associated with radiated waves) compared to quadratic damping (related to vortex shedding at the keel edges of the moonpool).

Driven by larger and larger water depths offshore Brazil and by the desire to develop heave-friendly floating platforms able to support Steel Catenary Risers, a mono-column concept has been developed by the University of Sao Paulo and Petrobras (see Ref [12]). This mono-column has a square outer cross-section and moonpool with a restriction at the keel of square shape as well. Radiation/diffraction analyses are performed with the WAMIT software (see Ref). Sensitivities to the restriction height and width are performed focusing on impact on heave motion RAOs. It is shown that decreasing the ratio of moonpool waterplane to keel restriction areas causes the RAO peak magnitude and period to decrease whilst additional peaks appear at longer periods. Radiation/diffraction calculations lack damping information causing heave RAOs to have peaks of unreasonable magnitude. Two mono-column configurations (moonpool dimensions not documented) were model tested. Free-surface decay tests in the moonpool are performed to assess damping level leading and obtain a reasonable fit with the peak of the measured heave RAO.

The MONOBR is a cylindrical version of the above-mentioned mono-column floater (see Figure 2-4). In Ref [13], analogy is made between a two body mass-spring-damping mechanical system and the two-body system consisting of the MONOBR floater and the water entrapped in its moonpool. The effect of a thin plate constriction at the bottom of the floater is investigated experimentally with a view to reducing the floater heave motion response. Model tests performed with fixed mono-column in waves shows that the piston mode natural period increases with decreasing opening at floater keel. Heave motion RAOs are derived for several keel opening diameters from measured signals and compared to two limit cases: a) keel is sealed and b) moonpool is unobstructed at keel. The single peak in case a) is replaced by two peaks in case b); one at a lower frequency and one at a higher frequency.

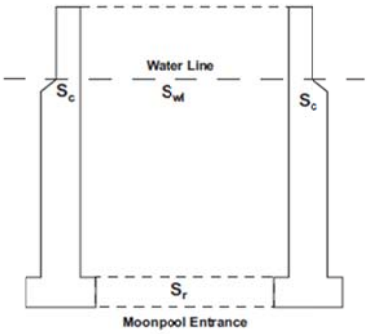

Figure 2-4 MONOBR elevation (from Ref [13])

The diameter of the keel opening affects the tested MONOBR heave motion response (both amplitude and frequency-wise). Whilst this is understandable for the hull shape shown in Figure 2-4 (owing to the large ratio of entrapped water mass to floater displaced mass), this influence on heave motion response is less likely to be noticeable when considering the volume of entrapped water in a turret compared to the FPSO displaced volume.

Radiation/diffraction software Hydrostar (see Ref [15]) is used in Ref [16] to investigate the wave elevation response in a truncated thin-walled cylinder. Two approaches are used to derive the RAO of the wave elevation at the centre of the cylinder: a) The potential method (with reference to the quantity being solved) also known as the direct method and b) the source method (again with reference to the quantity being solved) and also known as the indirect method. As shown below, refining the mesh density cause the period of peak response to increase in no marginal ways. The large peak values obtained are typical of a resonance phenomenon in the absence of damping.

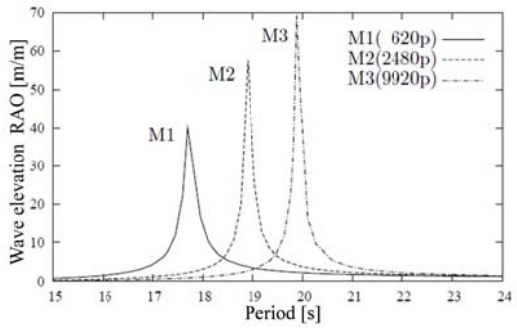

Figure 2-5 Wave elevation RAO in thin-walled truncated cylinder with potential method (from Ref[16])

A Multi-Domain approach is proposed in Ref [16] with a view to overcoming the abovementioned convergence problem. Application of this method (which is not yet implemented in commercially available Hydrostar) to the thin-walled cylinder problem leads to converging results with the coarsest of all three meshes (M1 in Figure 2-5). The converged resonance period is found at 18.5s which means that the potential method appears, for the thin-walled cylinder example, to converge asymptotically to a non-physical value.

3. RECENT TRENDS IN TURRET SYSTEM MOONPOOL DIMENSIONS

Over the last fifteen years, SBM has built a large variety of internal turret systems. The general trend in terms of turret dimension is an increase given the higher complexity to develop new fields and ever-increasing client demands. Figure 3-1 hereafter presents the evolution of internal turret characteristics provided by SBM since 1996 in terms of turret mass, diameter and mass of entrapped water in the turret.

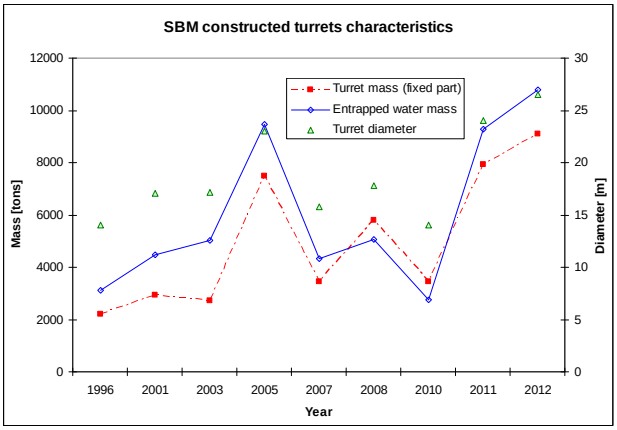

Figure 3-1: Track record of SBM turrets

Latest turret designs are today 3 to 4 times more massive than the systems designed fifteen years ago. The volume of entrapped water in the turret is so large that it is of primary importance to understand clearly the behaviour of this mass of water and its implications on loads applied to the bearings and various sloshing modes inside the moonpool. Sloshing of water inside the turret has also a direct influence on the elevation of radial wheels, hence on bearing loads.

4. INSIGHTS FROM RADIATION DIFFRACTION ANALYSIS

Time-domain or frequency domain mooring simulations for FPSOs, generally make use of frequency domain output from boundary element method (BEM) based linear radiation/diffraction software (e.g. AQWA-LINE, HydroStar, WAMIT, etc.). For first order solutions this output is generally either in the form of motion response amplitude operators (RAO) or alternately, wave load RAOs, added mass and damping frequency-dependent matrices. For second order solutions, quadratic transfer functions (QTF) are used.

In the light of the foregoing, it is a natural choice to attempt to model turret sloshing phenomena (i.e. loads and internal surface elevations) by means of radiation/diffraction software. Output from such model could then directly be incorporated in mooring simulations in the form of RAOs. However, modelling

turret moonpools in BEM based radiation/diffraction software is prone to mesh convergence issues as illustrated in the §2. Another issue is the insufficient ability to dampen resonant peaks in free surface elevation RAOs.

Following is a practical illustration of the issues encountered when using BEM based radiation/diffraction software to calculate surface elevation RAOs for a turret. In Figure 4-1, a simplified mesh of a turret is shown (a vertical symmetry plane has been used so that only 1/2 the turret is shown). In this model, there is no FPSO and the turret is fixed so that only the incident and diffracting problems are considered.

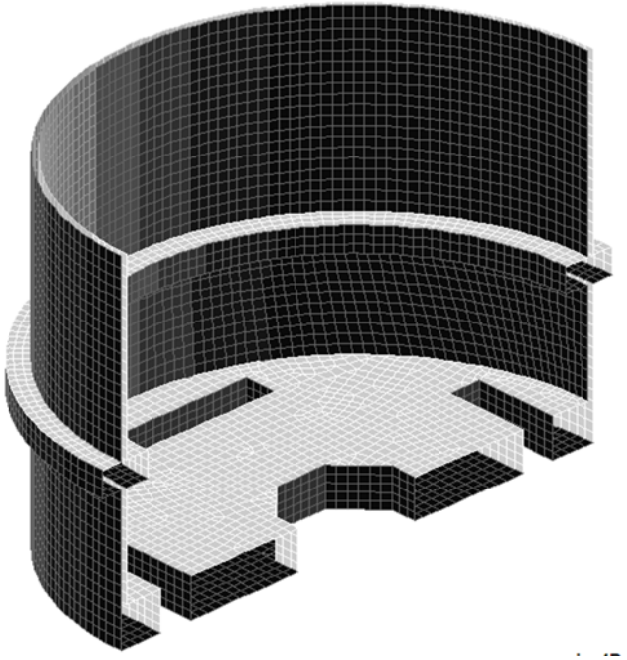

Figure 4-1 Turret mesh used with radiation/diffraction software.

The first task at hand is to recover the natural sloshing periods and to compute RAOs for the surface elevation inside the turret. To this end, three radiation/diffraction calculations were done with different panel sizes (number of panels for half geometry: 416, 1525, and 5154). The resulting surface elevation RAOs at the moonpool centre are shown as a function of wavenumber in Figure 4-2. It is immediately evident that the resonant peaks are a.) shifting towards lower wavenumbers with mesh refinement and b) too large to be physical (as for un-damped roll motion RAO's). Interestingly enough, the convergence trend for the McIver toroid mentioned in Ref [3] also appears to be present as illustrated in Figure 4-3). Other, more simplified meshes (for example, removing the rectangular openings (corresponding to openings near chain connectors) and ring-like box structure at the mid-level) have also been used, but have been found to yield qualitatively similar results.

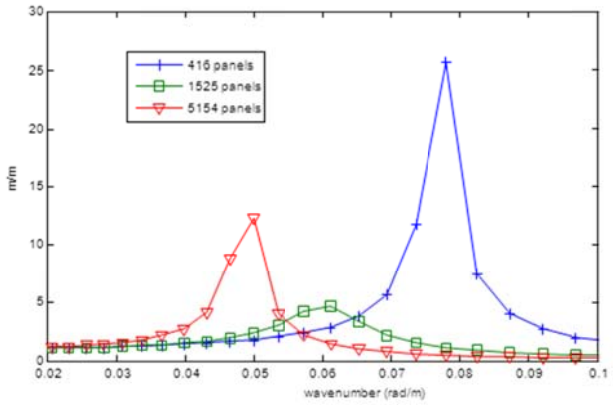

Figure 4-2 Surface elevation RAOs at the centre of the turret moonpool for meshes with different panel sizes

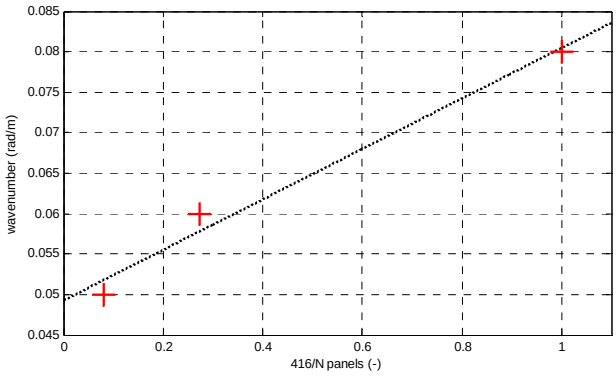

Figure 4-3 peak RAO wave-number as function of number of panels (crosses indicate wavenumber associated with RAO peaks, dotted line represents a least squares fit)

In the light of the foregoing, the applicability of BEM based radiation/diffraction software for turret sloshing problems has been found to be limited, thus calling for more complex numerical methods such as RANS solvers or model tests of course.

5. DYNAMICS OF ENTRAPPED WATER

Dynamics of entrapped water in a large internal turret have been assessed via Computational Fluid Dynamics simulations. Two different CFD solvers have been used, ISIS-CFD ([17]) the solver of the commercial package FINE™/Marine and COMFLOW ([18], [19]). Two kinds of simulations have been considered:

- Decay tests with a fixed turret in order to identify relevant natural oscillation modes of the water inside the turret;
- Forced heave oscillation of the vessel in still water to capture the flow dynamics and forces applied to the turret. This is considered to be a first step towards a more complete simulation including waves (with Froude-Krylov and diffraction effects included).

5.1 Presentation of COMFLOW

The COMFLOW program is one of the deliverables of the COMFLOW-2 JIP. COMFLOW is a program for the numerical simulation of fluid flow, based on Navier-Stokes equations. The program has been developed initially by the University of Groningen to study the sloshing of liquid fuel in spacecraft. In close co-operation with MARIN, the methodology was later extended to the calculation of green water loading on a fixed-bow deck and the analysis of anti-roll tanks.

The equations of fluid (conservation of mass and momentum) are solved with the help of a Volume Of Fluid methodology. The fluid is considered as a Newtonian fluid (viscosity accounted). Turbulence models are not incorporated in the model at the moment (it is planned to include turbulence models in a future release of the program). As the modelled fluid is Newtonian, the turbulence produced by the model is limited to a scale which is an order a magnitude greater than the local mesh size. Version 2.3 has been used.

5.2 Presentation of FINE™/Marine

FINE™/Marine is a finite volume, Reynolds-Average Navier-Stokes (RANS) CFD program that utilizes a Volume of Fluid (VOF) approach to track the free surface. FINE™/Marine is able to simulate floating body motions utilizing a six-degree of freedom solver and either rigid mesh motion or mesh deformation to cope with the body motions.

Turbulent flow is simulated by solving the incompressible Unsteady Reynolds-Averaged Navier-Stokes (URANS) equations. For the turbulent flow, additional transport equations for the modeled variables are discretized and solved. The two-equation SST k-ω linear eddy-viscosity model of Menter is used for turbulence modeling. A wall function is used to model the sublayer and a part of the log layer in the turbulent viscous layer.

5.3 Decay tests

The purpose of the free surface decay simulations is to identify the natural sloshing periods, both in the turret moonpool and the annular space. During the free surface decay tests, the free surface inside the turret/annular space is initially raised or inclined with respect to the mean surface level outside the vessel after which the surface is allowed to oscillate freely until a number of cycles has been recorded. Two types of free surface simulations were performed, a piston mode free surface decay tests in which the water moves up and down, and a sloshing mode free surface decay test in which the water moves back and forth from one side of the turret/annular space to another. The principle is illustrated in Figure 5-1 below.

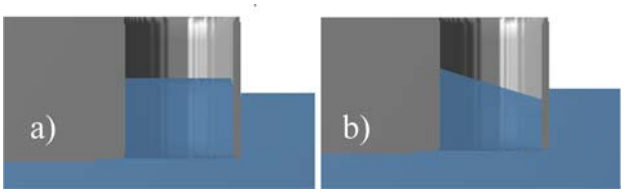

Figure 5-1: Initial liquid configuration for decay tests: a) piston mode decay – b) sloshing mode decay

The decay tests have been performed with two different numerical models:

- An accurate 14-million hexahedral elements mesh to be used with FINE™/Marine. A view of the surface mesh is given in Figure 5-2. The first cell (near the wall) height was sized to yield a y^+ of 200 at the peak velocities during the piston mode based on an estimate of a Blasius flat plate. Mesh size and time step sensitivity analyses have been performed to show spatial and temporal convergence. The refined mesh was generated with the elements at the turret free surface and chaintable refined to be half the size in each direction of the original mesh cells. A time step of half the original time step was used for temporal convergence. The results were found to be converged in both space and time.

- A coarse 1.8-million hexahedral element structured mesh to be used with COMFLOW solver. The COMFLOW mesh was prepared as a benchmark of the large model calculations. Chaintable openings have been done to reproduce the global porosity of the accurate model.

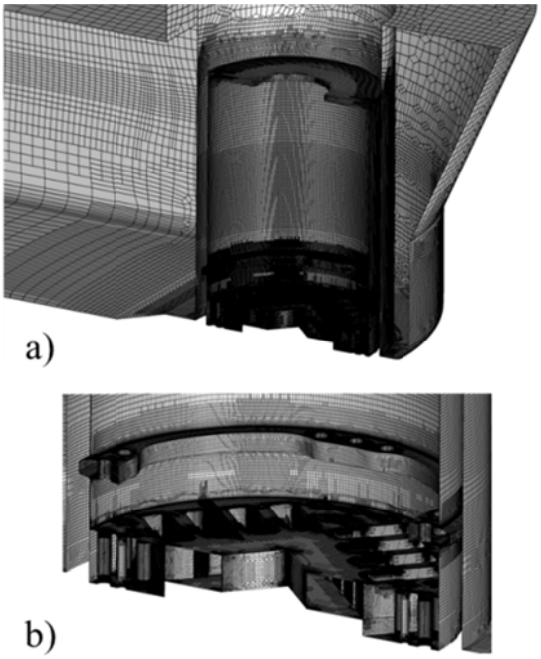

Figure 5-2: View of the detailed surface mesh prepared for FINE™/Marine solver: a) Bow section; b) Chaintable

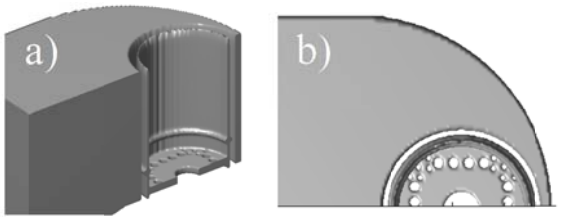

Figure 5-3: View of the coarse geometry prepared for COMFLOW solver: a) Isometric view b) bird eye view with chaintable openings

The simulations have been run and resulting time series of water level in the turret and in the turret annulus are presented on Figure 5-4 and Figure 5-5 for the piston decay test and on Figure 5-6 and Figure 5-7 for the sloshing decay test.
A very accurate agreement is found between the two approaches for all cases except for the sloshing mode inside the turret (natural sloshing period in the turret is found shorter in the COMFLOW simulations). This is explained by the fact that due to the Cartesian grid requirement for COMFLOW solver, turret cylinder thickness must be increased compared to reality in order to obtain a continuous turret cylinder free of artefacts and mesh defects.

Computed natural periods have been compared with theoretical formulations found in the literature (Ref [20]) and show a very good agreement as well, see Table 5-1 hereafter.

Piston mode	Natural period annulus [s]	Natural period turret cylinder [s]*
Analytical	8.9	13.1
COMFLOW	9.6	12.4
FINE™/Marine	9.6	12.4
Sloshing mode	**Natural period annulus [s]**	**Natural period turret cylinder [s]***
Analytical	7.4	5.8
COMFLOW	7.4	5.4
FINE™/Marine	7.5	5.6

Table 5-1 Piston & Sloshing mode natural periods

For the sloshing mode, it has also been found that flows in the turret and in the turret annulus do not influence mutually each other (water velocities at the bottom of the turret are very low in this case). Influence between turret and annulus is also limited in the case of the piston mode, but still exists. Significant viscous damping of turret water level is found for the piston mode due to vortex generation from flow through the chaintable openings as shown in Figure 5-8.

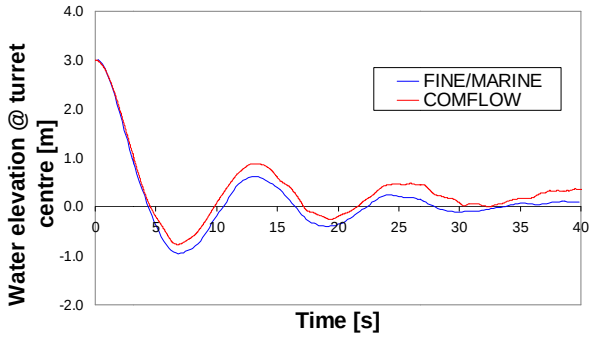

Figure 5-4: Piston decay test - Comparison of COMFLOW vs FINE™/Marine - Results @ turret centre

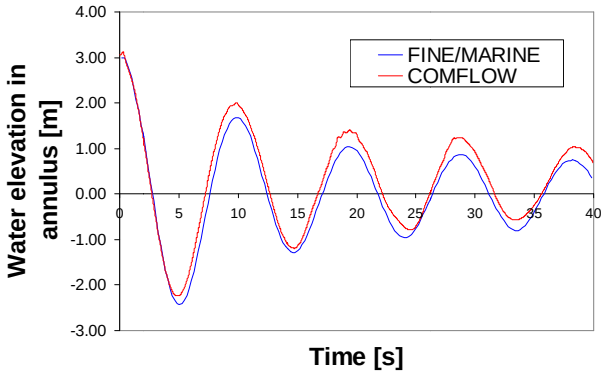

Figure 5-5: Piston decay test – Comparison of COMFLOW vs FINE™/Marine - Results in turret annulus

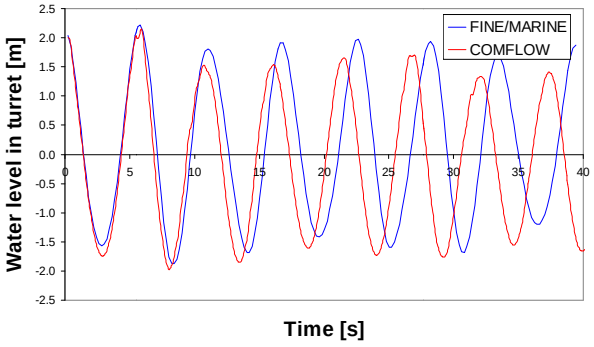

Figure 5-6: Sloshing decay test - Comparison of COMFLOW vs FINE™/Marine - Results at a radius of 12m in turret

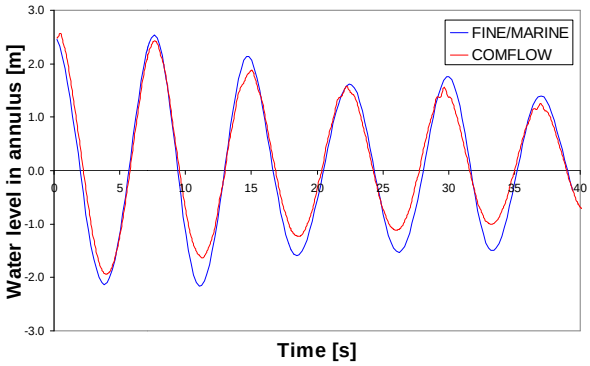

Figure 5-7: Sloshing decay test – Comparison of COMFLOW vs FINE™/Marine – Results in turret annulus

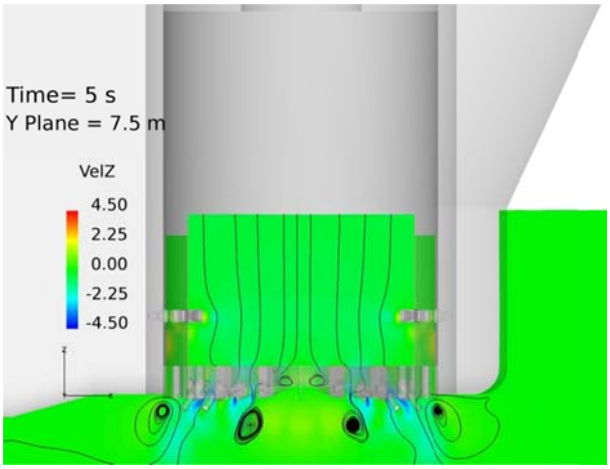

Figure 5-8: Vortex generation from flow through chain table, Y plane = 7.5 m

As previously mentioned, vessel forced-heave oscillations tests have been performed as well with FINE™/Marine. The results of these calculations will be reported in a future publication. Forced-heave calculations could not be run with COMFLOW due to the following limitations:

- Unexplained spikes were obtained on the force time series with no clear means of removing them apart from low-pass filtering;
- Convergence was very difficult to reach on models having a large number of cells (>4 million cells). This caused the solver to increase the number of temporal iterations within each time step. No workable solution could be found.

6. ENTRAPPED WATER AND TURRET LOADS

Water entrapped in the turret moonpool will cause additional loads on the turret weathervaning system; when the turret undergoes motions, the water entrapped inside the turret will attempt to resist motion (i.e. inertia). Additionally, the entrapped water will have a tendency to undergo a periodic motion (i.e. sloshing) when excited by the turret motion or by direct wave action. It is of importance to understand the degree to which the loads associated with entrapped water coincide with other load components (primarily those associated with the mooring and riser systems).

A first indication of the magnitude and phasing of loads from entrapped water can be obtained from thinking of the water in the turret moonpool as a fixed mass of water (e.g. "frozen"). This will cause entrapped water loads that are out of phase with turret acceleration. From time-domain mooring output, instances of maximum turret load events can be identified, and the associated accelerations around these events can be found.

As an example, in Figure 6-1 and Figure 6-2, output from time-domain simulation of a large turret-moored FPSO dynamics is shown. The vertical position and acceleration of the turret are plotted in the vicinity of an extreme turret vertical load event (indicated by the red vertical line in the abovementioned figures). From the time domain analysis, it is known that the turret loads at the time of the extreme primarily originate from the mooring and riser systems.

The global (over the entire simulation) minima and maxima of motions/accelerations are indicated in the figures by the horizontal dotted lines. It is clear from the figures that the minima and maxima of turret position and acceleration almost coincide with the time of the extreme turret vertical load event. When using the "frozen" water assumption for the entrapped water, loads from entrapped water will nearly be maximized for this turret load event, underscoring the need of taking the entrapped water effects into account. Furthermore, it can be seen that the period of motion ahead of the extreme turret load event is around 16s. This period is relatively close to the piston mode period shown in Table 5-1. This underlines the necessity of identifying the natural sloshing periods and understanding corresponding levels of damping when excitation is close to resonance.

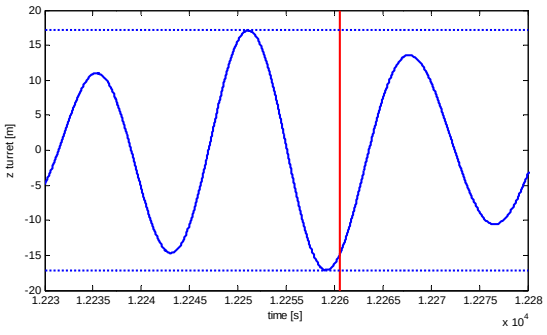

Figure 6-1 Vertical turret position in the vicinity of extreme turret load event (red vertical line). Horizontal dotted lines indicate 3-hour vertical position extremes.

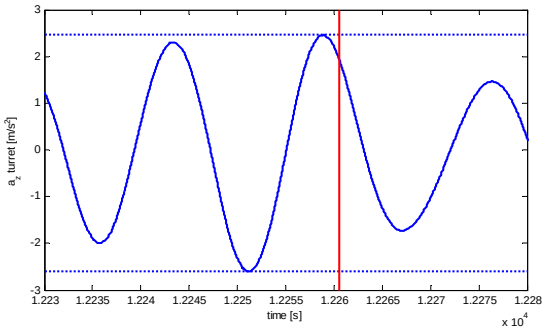

Figure 6-2 Vertical turret acceleration in the vicinity of extreme turret load event (red vertical line). Horizontal dotted lines indicate 3-hour vertical acceleration extremes.

Vertical turret loads from entrapped water are primarily a result of pressure differences between the chaintable top and bottom faces. The following components are at play:
Above the chaintable:

A1. Hydrostatic pressure; the pressure at the top of the chaintable associated with the water column height above;

A2. Dynamic pressure; momentum change (i.e. $\frac{d}{dt}(mV)$) of the time-dependent mass of entrapped water in the turret moonpool causes pressure variations at the top of the chaintable.

Below the chaintable:

B1. Hydrostatic pressure; the pressure below the chaintable varies with its depth below the free surface.

B2. Dynamic pressure; the pressure at the bottom of the chaintable due to time varying wave pressure.

Thus, turret loads are influenced by the amount of water in the turret moonpool, by the variation of that amount (i.e. the $V.\frac{d}{dt}(m)$ term) and by the motion of the turret itself. The variation of the amount of water is due to turret motions relative to waves and due to the piston-mode effects. It is therefore important to understand both the magnitude and phasing of sloshing effects.

As mentioned above, the modelling of the variation of the mass of entrapped water, and the loads associated with the movement of the water in the turret has so far proven beyond the capability of state-of-the-art BEM-based radiation/diffraction software.

Under motion in waves, it is evident that the total load will be determined by the magnitude and phasing of the individual components.

7. PRACTICAL IMPLEMENTATION AND GUIDELINES

With the trend of increasing turret and mooring system sizes, the joint occurrence of extreme sloshing and other loads (mooring system, turret hydrostatics, weight and inertia) can increasingly affect design parameters; turret loads have already been mentioned, but other areas may also be affected by sloshing, for example buckling loads due to pressure differences between the inside and outside of the turret, free surface velocities inside the turret that could conceivably hinder the installation process or cause pressure peaks on sensitive equipment. For some turret projects, labyrinths have been mounted in the annulus space to reduce water level fluctuations in this semi-enclosed space. The presence of friction pads may remedy partly the abovementioned fluctuations. In summary, investigation of loads from sloshing phenomena in mooring simulation, either directly or indirectly through post-processing, is highly recommended.

At present, BEM based radiation/diffraction software has a number of associated issues which limit its applicability to turret sloshing problems. More advanced methods such as RANS based CFD can provide valuable insight in turret sloshing issues, but due to large computational requirement, they are not practicable for time-domain mooring simulations in irregular waves.

Therefore, for the inclusion of sloshing phenomena in turret moonpools, the following approach is proposed:

- Usage of a simplified model in time domain mooring simulation (a first approach would be to consider the water entrapped in the turret moonpool as “frozen”);
- Verification of the loads obtained from time-domain simulation by a limited number of CFD simulations (e.g. imposed motion simulation in regular waves).

Should model tests be performed, it is highly recommended to include measurements of relative wave elevations at three suitable locations in the turret moonpool. The scale model of the moonpool shall be constructed to be as representative as possible of the actual geometry.

8. CONCLUSIONS

The increase in the volume of entrapped water in recent turret systems raises the concern about its behaviour when the FPSO-mounted turret is subjected to large first order motions and the chaintable is loaded by wave-induced dynamic pressure. This behaviour is of interest for two main reasons: a) to what extent dynamics of entrapped water affects the global loads exerted on the turret weathervaning system (axial bogies and radial wheels in Figure 1-1) and b) to what extent sloshing in the turret can lead to run-up along annulus walls (in the absence of

labyrinth) or turret moonpool walls and damage to sensitive equipment.

The BEM-based radiation/diffraction models of turret moonpools are not able to capture with enough accuracy the resonant periods in general and the piston mode natural period in particular.

With model test facilities often not readily available at short notice, alternative investigation means are required to develop the turret design and confirm the validity of the adopted numerical analysis methodology. In this paper, the benefit of CFD is demonstrated through examples of free surface decay simulations in a turret moonpool and turret annulus. Good consistency in the prediction of piston and sloshing natural periods is found between two CFD programs despite drastic differences in mesh complexity, level of details and CPU time.

9. ACKNOWLEDGEMENTS

The authors would like to thank the SBM Offshore execution centre and its Proposal/Technology Development branch for their unwavering and continuous support and for the authorization to present highlights of recent CFD advances.

10. REFERENCES

[1] "Coupled CFD Simulation of the Response of a CALM Buoy in Waves" by P. Woodburn. P. Gallagher, M. Naciri and J.-P. Borleteau. *Proceedings of the 24th International Conference on Offshore Mechanics and Arctic Engineering.* (2005) Halkidiki Greece

[2] "Resonance in the unbounded water wave problem" by M. McIver. *Proceedings of the 12th IWWWFB* (1997) Carry-le-Rouet France.

[3] "Hydrodynamic analysis of the McIver toroid" by J.N. Newman. *Proceedings of the 13th IWWWFB* (1998) Alphen Van den Rijn The Netherlands.

[4] "Radiation and diffraction analysis of the McIver toroid" by J.N. Newman *Journal of Engineering Mathematics* (1999) **35** pp135-147.

[5] "The MFB, a Deep Water FPSO with Surface Trees and Drilling Facilities", By C. Valenchon, J.H. Rossing, G. Pouget, and F. Biolley *Proceedings of the Offshore Technology Conference* (1998) Reference on the multi-function barge.

[6] "A Surface Tree Riser Tensioning System for FPSOs" by J. Pollack, L. Poldervaart & M. Naciri. *Proceedings of the Offshore Technology Conference* (2000) Paper OTC 11902 Houston Texas U.S.A

[7] "On the piston mode in moonpools" by B Molin *Proceedings of the 14th IWWWFB* (1999) Port Huron Michigan U.S.A.

[8] "Piston and sloshing modes in moonpools" by B Molin *J. Fluid. Mech.* (2001) Vol. 430, pp. 27-50.

[9] "Low-frequency resonance of moonpools" by J.N. Newman. *Proceedings of the 18th IWWWFB* (2003) Le Croisic France.

[10] "Flow dynamics in a moonpool. Experimental and numerical assessment" by C. Maisondieu & M. Le Boulluec *Proceedings of the 20th International Conference on Offshore Mechanics and Arctic Engineering*. (2001) Rio de Janeiro, Brazil.

[11] "Simulation bidimensionnelle des écoulements dans une baie de forage. Etude des modes de résonance et des amortissements" by C. Maisondieu, B. Molin, O. Kimmoun and L. Gentaz. *8èmes Journées de l'Hydrodynamique (in French)* March 5th-7th (2001) Nantes, France.

[12] "Study of Numerical Modeling of Moonpool as Minimization Device of Monocolumn Hull" by F.G.S. Torres, M. Cueva, E. B. Malta, K. Nishimoto and Marcos D. Ferreira *Proceedings of the 23rd International Conference on Offshore Mechanics and Arctic Engineering*. Paper 51540 (2004) Vancouver, British Columbia, Canada.

[13] "Monocolumn behaviour in waves: Experimental analysis" by S.H. Sphaier, F.G.S. Torres, I.Q. Masetti, A.P. Costa and C. Levi *Ocean Engineering* 34 (2007) pp1724-1733.

[14] WAMIT® User Manual Version 7.0 - Updated for version 7.02 - April 2012.

[15] Hydrostar for Experts – User Manual - June 2012.

[16] "Multi-Domain Boundary Element Method with Dissipation", by Chen, X., Duan, W. *Journal of Marine Science and Application*, (2012), Vol 11, Issue 1, pp 18-23.

[17] "An interface capturing method for free-surface hydrodynamic flows," by P. Queutey, and M. Visonneau *Computers & Fluids* (2007), Vol. 36, pp. 1481–1510.

[18] "Modelling two-phase flow with offshore applications", by Wemmenhove, R., Loots, G.E., Luppes, R., Veldman,A.E.P., *24th Offshore Mechanics and Arctic Engineering Conference*, paper 67460, (2005) Halkidiki, Greece.

[19] "COMFLOW Manual V2.3", by Wemmenhove, R., Loots, G.E., Luppes, R., Veldman,A.E.P., Wellens P., Bunnik T., Helmholt-Kleefsman T., COMFLOW-2 JIP Project, MARIN Reference 18378, (2008).

[20] "Environmental conditions and environmental loads", Recommended Practice, Det Norske Veritas, DNV-RP-C205, October 2010.

